HYDRODYNAMIC REGIMES OF A LIQUID IN A SMOOTH-WALLED ROTATING HEAT PIPE. 1

M. G. Semena and Yu. A. Khmelëv

UDC 532.542

The article presents the results of the analytical and experimental investigation of the hydrodynamics of a liquid in a horizontal rotating heat pipe. A formula is derived for determining the thickness of the layer of liquid entrained from the groove of the inner cylindrical surface.

Heat exchange in smooth-walled rotating heat pipes (RHP) has a number of special features compared with the heat exchange in fixed natural-circulation pipes, chiefly on account of the effect of the rotational speed on the distribution of the layer of liquid on the inner surface of the RHP. By determining the nature of the distribution and of the flow of liquid in the inner cavity of the RHP, we can explain the phenomenon of hysteresis of the heat transfer coefficient in the zone of the condensation [1], the complex nature of the dependence of the heat transfer coefficient in the zone of evaporation [2] and of the heat-transferring ability of the RHP on the rotational speed [3]. Up to the present, practically no detailed study has been carried out of the distribution of the heat carrier in an RHP for a broad range of rotational speeds. The attempt at visual investigation [4] is of a partial nature.

The aim of the present work is to study the hydrodynamics of a liquid in an RHP in dependence on the rotational speed, the geometric characteristics of the pipe, the physical properties of the heat carrier, and its quantity. The object of investigation is a cylindrical RHP, situated horizontally and rotating with constant angular velocity ω about the longitudinal axis. The angle φ is measured anticlockwise from the upper generatrix. On condition that the volume V filled with liquid is uniformly distributed, a layer forms on the inner surface of the RHP whose thickness is $\bar{\delta}$, and $\delta/R \ll 1$.

The equation of continuity and of conservation of momentum in cylindrical coordinates in the approximation of the boundary layer, written with a view to the new variable $\varepsilon = R - r$, has the form

$$\frac{1}{R-\varepsilon}\frac{\partial v_\varphi}{\partial \varphi} - \frac{\partial v_\varepsilon}{\partial \varepsilon} = 0, \tag{1}$$

$$\frac{1}{\rho(R-\varepsilon)} v_\varphi \frac{\partial v_\varphi}{\partial \varphi} = -\nu\left[\frac{\partial^2 v_\varphi}{\partial \varepsilon^2} - \frac{1}{R-\varepsilon}\frac{\partial v_\varphi}{\partial \varepsilon} - \frac{v_\varphi}{(R-\varepsilon)^2}\right] - g\sin\varphi. \tag{2}$$

The results of the numerical solution of Eqs. (1) and (2), carried out by using various methods [5, 6], agrees well with the experimental data obtained by us. In generalized form they may be presented in the form of the graph shown in Fig. 1, which illustrates the existing flow regimes in dependence on the rotational speed, the radius of the inner surface, the viscosity of the liquid and its amount. The experimental investigation was carried out with an installation that was additionally equipped with a device for measuring the thickness of the layer of liquid by the method of electric contact. To make the flow visible, one of the end faces of the stainless steel pipe (D_{in} = 64 mm, l = 300 mm) was made of glass. The working liquid was water and methyl alcohol.

The position of the free surface of the liquid in an RHP depends on the flow regime and is determined by the angular coordinate of the maximum thickness of the layer φ_m and the ratio $\xi = \delta_m/\bar{\delta}$. There exist two limit flow regimes: the region of "rotation of a solid" and and the region of the "entrained thin layer." Between them there are two transitional regimes: the regions of viscous flow and of inertia flow.

50th-Anniversary-of-the-Great-October-Socialist-Revolution Kiev Polytechnic Institute. Translated from Inzhenerno-Fizicheskii Zhurnal, Vol. 43, No. 5, pp. 766-774, November, 1982. Original article submitted July 21, 1982.

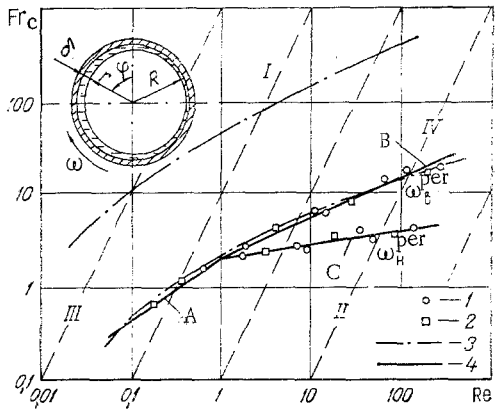

Fig. 1. System of coordinates and nomograph of flow regimes of a liquid: I) region of "rotation of a solid"; II) region of "entrained thin layer"; III) region of viscous flow; IV) region of inertia flow; 1) water; 2) methyl alcohol; 3) numerical calculation [5]; 4) present work; A (3)) $Fr_c = 2.2Re^{0.77}$; B (4)) $Fr_c = 2.2Re^{0.44}$; C (5)) $Fr_c = 2.2Re^{0.13}$, $Fr_c = \omega^2 R/g$; $Re = \omega(\bar{\delta})^2/\nu$.

The region of rotation of a solid I is situated in the left-hand upper corner of the graph. In this region the liquid is distributed practically uniformly over the surface ($\xi = 1$) and moves with constant speed $v_\varphi \approx \omega R$. This regime applies when, with low Fr_c numbers, the liquid is sufficiently viscous or its quantity is small, i.e., the Re number is small, or when with high Re numbers, the Fr_c number is also high. In the former case the viscous forces predominate throughout the thickness of the layer of liquid δ, in the latter case only in the boundary layer $\delta_{boun} \ll \bar{\delta}$ next to the wall, the thickness of the boundary layer decreasing with increasing rotational speed. On the motion of the liquid outside the boundary layer, vibrations due to the force of gravity are superimposed, the amplitude of the vibrations tending to zero with increasing Fr_c.

The region of the entrained thin layer II, situated in the right-hand lower corner of the graph, is characterized by the existence of a groove in the lower part of the RHP and of a thin layer of liquid on the remaining surface, and it is encountered when the Fr_c numbers are small or the Re numbers are large (low viscosity of the liquid or a large amount of it). In these cases neither the viscous nor the inertial forces are able to ensure distribution of the liquid without some rest in the form of a groove. That most of the surface is covered by a film is due to the entrainment of the liquid from the groove by the wall.

The region of viscous flow III is situated in the left-hand lower corner of the graph, where the Fr_c and Re numbers are small, i.e., the viscous and gravitational forces predominate over the forces of inertia. Here the viscosity effect spreads across the entire thickness of the layer of liquid, independently of the magnitude of Fr_c. The speed of the liquid, running down under the effect of the force of gravity, is commensurable with the linear velocity of the wall. The mean speed of the flow on the descending part of the pipe is higher than on the rising part, therefore the layer is thicker on the latter side ($\xi > 1$). The maximum value of ξ corresponds to the instant when the speed of the free surface at the point $\varphi = \pi/2$ is close to zero. The angular coordinate of the maximum thickness of the layer δ_m in this regime remains practically constant and equal to $\varphi = \pi/2$.

The region of inertia flow IV is situated in the right-hand upper corner of the graph and is characterized by relatively high Fr_c and Re numbers. Here the viscous forces have an effect only in a thin boundary layer near the wall. This is encountered when the liquid has low viscosity or when its amount is large. The flow velocity of the free surface varies with a period of 2π relative to the mean value that is approximately equal to ωR, and it attains its maximum in the lower part of the pipe, its minimum in the upper part. Thus, in the upper part of the RHP the layer of liquid is thicker ($\xi > 1$) than in the lower part. The angular position of δ_m is close to $\varphi = 0$.

In transition from region IV to region III, the angular position of the magnitude of δ_m changes from $\varphi = 0$ to $\varphi = \pi/2$, and in transition from region I to region II, the magnitude of ξ increases from $\xi = 1$ to ξ_{max}. The point characterizing the flow regime in the RHP moves along the straight lines which in the graph are indicated by dashed lines. The given slope of these straight lines is due to the fact that the Reynolds number is a function of ω, and the centrifugal Froude number is a function of ω^2. Thus, when the rotational speed changes (shift along the above-mentioned lines), both ξ and the angular coordinate φ_m change.

Experimental investigation also showed that there is some hysteresis of the process of transition from region II to region IV for numbers $Re > 1$. The hysteresis is due to the fact that upon emergence of the flow regime from region II by increasing the rotational speed up to ω_H^{per} (Fig. 1) the process of entrainment of the liquid by the wall does not yet ensure its distribution over the linear surface without some rest in the lower part of the pipe. The groove prevents laminar flow of the layer of liquid with the maximum speed of the free surface in the lower part of the pipe, i.e., it prevents the regime of inertia flow; if this groove is to disappear completely, the speed must be increased to some values ω_B^{per}. In the opposite transition from region IV to region II by reducing the speed, the regime of inertia flow is maintained up to the speed ω_H^{per}.

Generalizing the experimental data and the results of numerical calculation, we can determine quantitatively the boundaries of the existing flow regimes. For region III ($Re < 1$) the boundary of the transition to region II (the straight line A in Fig. 1) is approximated by the equation

$$Fr_c = 2.2\,Re^{0.77}. \tag{3}$$

For region IV ($Re > 1$), the upper (straight line B) and lower (straight line C) boundaries of the transition to region II in the zone of hysteresis are determined, respectively, by the equations

$$Fr_c = 2.2\,Re^{0.44}, \tag{4}$$

$$Fr_c = 2.2\,Re^{0.13}. \tag{5}$$

Equations (3), (4), and (5) are applicable to the region: $0.05 < Re < 500$. There is no distinct boundary of transition to region I because with increasing Fr_c number ξ approaches unity monotonically. In Fig. 1 the arbitrary boundary of region I, corresponding to $\xi = 1.01$, is shown

The distribution of the liquid over the inner surface of the RHP, i.e., the function $\delta = f(\varphi)$, for the regimes in the regions I, III, and IV can be found relatively simply. Thus, for region I this function degenerates to the equality $\delta(\varphi) = \bar{\delta} = \text{const}$. For regime III it is found by integrating the equation of motion in which we neglect the effect of the forces of inertia and of surface tension:

$$\nu\left[\frac{\partial^2 v_\varphi}{\partial \varepsilon^2} - \frac{1}{R-\varepsilon}\frac{\partial v_\varphi}{\partial \varepsilon} - \frac{v_\varphi}{(R-\varepsilon)^2}\right] = -g\sin\varphi, \tag{6}$$

and the continuity equation in the form

$$-\omega R\bar{\delta} = \int_0^\delta v_\varphi d\varepsilon = \text{const}. \tag{7}$$

To determine the function $\delta = f(\varphi)$ in region IV, we may use the model of [5] according to which the layer of liquid is divided into the near-wall region, in which the layer of liquid forms on account of the difference is speed of the principal flow of liquid and of the wall, and into the region bounded by the free surface where the change of speed occurs under the effect of the gravitational forces. The respective equations of motion for these two regions have the form

$$\frac{\partial v_\varphi}{\partial t} = \nu\frac{\partial^2 v_\varphi}{\partial \varepsilon^2}, \tag{8}$$

$$\frac{\partial v_\varphi}{\partial t} = -g\sin\omega t. \tag{9}$$

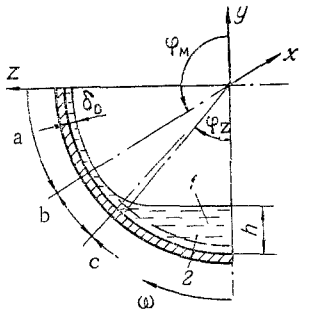

Fig. 2. The process of entrainment of a liquid by the inner surface of a cylindrical pipe: a) zone of entrainment; b, c) zones of dynamic and static meniscus, respectively; 1) groove; 2) near-wall annular layer of liquid.

Then the function $\delta = f(\varphi)$ for regime IV is found by integrating Eqs. (8) and (9), and then the continuity equation (7) with the corresponding boundary conditions applying.

The distribution of the liquid over the inner surface of the RHP in region II is described by a more complex function and requires detailed examination. To analyze the processes of hydrodynamics in the region, we subdivide the layer of liquid next to the wall, moving upwards, into three zones (Fig. 2): 1) the zone of entrainment a, situated fairly far above the level of liquid in the groove (here the thickness of the layer is practically constant over the angle φ because the mean flow velocity is close to the linear velocity of the wall); 2) the zone of the dynamic meniscus b, where the meniscus, forming under the effect of the forces of surface tension, is deformed by the motion of the wall (the liquid in this zone moves much more slowly than in the preceding one, but the change of speed, and consequently also the change of thickness of the layer, are considerable); 3) the zone of the static meniscus c, where the liquid moves at such low speed that this speed may be neglected and that it may be assumed that the shape of the free surface is determined solely by the forces of surface tension, like in the case of the meniscus of a motionless surface.

The equation of motion for the second zone (b) and the equation of the static meniscus for the third zone (c) have the form:

$$v_\varphi \frac{1}{R-\varepsilon}\frac{\partial v_\varphi}{\partial \varphi} = \frac{1}{R-\varepsilon}\frac{\partial P}{\partial \varphi} - \mu\left[\frac{\partial^2 v_\varphi}{\partial \varepsilon^2} - \frac{1}{R-\varepsilon}\frac{\partial v_\varphi}{\partial \varepsilon} - \frac{v_\varphi}{(R-\varepsilon)^2}\right] - \rho g \sin\varphi, \tag{10}$$

$$\frac{\sigma}{R_{cr}} = -g\rho H_м. \tag{11}$$

If we substitute the expression for the radius of curvature in the orthogonal coordinate system into Eq. (11), we obtain:

$$\frac{\frac{d^2z}{dy^2}}{\left[1+\left(\frac{dz}{dy}\right)^2\right]^{3/2}} = \frac{y+R-h}{a^2}. \tag{12}$$

The boundary conditions for Eq. (12) are:

$$\left.\frac{dz}{dy}\right|_{y=h-R} = -\infty. \tag{13}$$

We write Eq. (12) in the cylindrical coordinate system:

$$\frac{\delta''(R-\delta)+2(\delta')^2-(R-\delta)^2}{[(R-\delta)^2+(\delta')^2]^{3/2}}=\frac{(R-\delta)\cos\varphi}{a^2}+\frac{R-h}{a^2}. \tag{14}$$

If we integrate Eq. (12) with the boundary conditions (13), we obtain:

$$\frac{R\cos\varphi-\delta'\sin\varphi-\delta\cos\varphi}{[(R-\delta)^2+(\delta')^2]^{1/2}}=\frac{(R-\delta)^2\cos^2\varphi}{2a^2}+\frac{(R-h)(R-\delta)\cos\varphi}{a^2}+\frac{(R-h)^2}{2a^2}-1. \tag{15}$$

We determine the conditions which Eqs. (14) and (15) have to satisfy in the transition region to the thin layer of liquid, i.e., in the upper part of the zone of the dynamic meniscus. The thickness of the layer here is small, and it tends to some value δ_0 which we shall call the thickness of the entrained layer. The first derivative of the thickness of the layer with respect to the angle φ then tends to zero:

$$\delta'=0 \quad \text{for} \quad \delta=\delta_0. \tag{16}$$

From Eq. (15) we determine the value of φ_M at which condition (16) is satisfied, and this we substitute into Eq. (14). We obtain:

$$\delta''=\frac{(R-\delta_0)^2[(R-\delta_0)\cos\varphi_M+(R-h)]}{a^2}-(R-\delta_0), \tag{17}$$

where

$$\cos\varphi_M=\{a^2-(R-h)(R-\delta_0)+$$
$$+\sqrt{[-a^2+(R-h)(R-\delta_0)]^2-(R-\delta_0)^2(R-h)^2+2a^2(R-\delta_0)^2}\}\{(R-\delta_0)^2\}^{-1}.$$

Thus, when conditions (16) and (17) are satisfied, the solution of the equation of the static meniscus changes into the solution of the equation of the dynamic meniscus.

In the known solutions of the problem of the entrainment of a liquid from an unbounded volume by a moving flat surface a different approach was used in taking into account the effect of the forces in Eq. (10) and in its solution. For instance, the solution in [8] taken into account all the forces: of inertia, viscous, gravity, and the change in pressure under the effect of the force of surface tension; in the solution [9] the forces of inertia are neglected. Analysis and experimental verification of [8] showed that this solution yields the best agreement with the experimental data. However, when the capillarity numbers $Ca < 0.03$, the solution of [9] practically coincides with that of [8] and with the experiment.

Taking it that for the operating conditions of an RHP $Ca < 10^{-2}$, we neglect the effect of inertia. Then Eq. (10) in the approximation of the boundary layer assumes the form

$$0=\frac{\sigma}{R^3}\frac{\partial^3\delta}{\partial\varphi^3}-\mu\left[\frac{\partial^2 v_\varphi}{\partial\varepsilon^2}-\frac{1}{R-\varepsilon}\frac{\partial v_\varphi}{\partial\varepsilon}-\frac{v_\varphi}{(R-\varepsilon)^2}\right]-\rho g\sin\varphi. \tag{18}$$

We integrate Eq. (18) with the boundary conditions:

$$v_\varphi=\omega R \quad \text{for} \quad \varepsilon=0,$$

$$\frac{\partial}{\partial\varepsilon}\left(\frac{v_\varphi}{R-\varepsilon}\right)=0 \quad \text{for} \quad \varepsilon=\delta. \tag{19}$$

As a result of this and taking into account the condition $R \gg \delta$, we determine the speed of the liquid in the layer:

$$v_\varphi=-\omega R+\left(-\frac{\sigma}{\mu R^3}\delta'''-\frac{\rho g\sin\varphi}{\mu}\right)\left(\frac{\varepsilon^2}{2}-\delta\varepsilon\right). \tag{20}$$

If we substitute (20) into the continuity equation

$$-\omega R\delta_0=\int_0^\delta v_\varphi d\varepsilon=\text{const}, \tag{21}$$

we obtain:

$$\omega R\delta_0 = \omega R\delta + \left(\frac{\sigma}{\mu R^3}\delta''' - \frac{\rho g \sin\varphi}{\mu}\right)\frac{\delta^3}{3}. \tag{22}$$

We find the solution of Eq. (22) with the boundary conditions

$$\left.\begin{array}{l}\delta \to \delta_0,\\ \delta' \to 0,\\ \delta'' \to 0,\end{array}\right\} \quad \varphi \to 0. \tag{23}$$

We find the sought value of δ_0 from the condition of joining the soulution of Eq. (22) with the solution of Eq. (14) by the method of [9]. The condition of joining is

$$R_{cr}^{st}|_{\delta\to\delta_0} = R_{cr}^{d}|_{\delta\to h}, \tag{24}$$

where R_{cr}^{st}, R_{cr}^{d} are the radii of the curvature of the surface determined from the equations of the static (14) and of the dynamic (22) meniscus, respectively.

If we use the expression for the radius of curvature in the cylindrical coordinate system, Eq. (17), and the condition $R \gg \delta$, we obtain

$$R_{cr}^{st}|_{\delta\to\delta_0} = -\frac{a^2}{R\cos\varphi_M + (R-h)}. \tag{25}$$

For determining the value of $R_{cr}^{d}|_{\delta\to h}$ we find the value of δ'' from Eq. (22) for $\delta\to h$ with the aid of the numerical solution, using the "viscous-surface" approach of [9], and taking the boundary conditions (23) into account, we have:

$$\delta'' = 1.34R^2\frac{Ca^{2/3}}{\delta_0}. \tag{26}$$

Then, using the expression for the radius of curvature in the cylindrical coordinate system, Eq. (26), and the condition $R \gg \delta$, we find:

$$R_{cr}^{d}|_{\delta\to h} = -\frac{R^2}{1.34R^2\dfrac{Ca^{2/3}}{\delta_0} + R}. \tag{27}$$

If we substitute (25) and (27) into (24), we obtain an expression for determining the thickness of the layer of liquid entrained by the cylindrical wall in dependence on the rotational speed, the radius of the pipe, the physical properties of the liquid and its amount, determined by the depth h of the groove:

$$\delta_0 = 1{,}34\frac{RCa^{2/3}}{\sqrt{\dfrac{2hR}{a^2} + 1}}. \tag{28}$$

If we substitute into (28) the conditions characterizing the process of entrainment of a liquid by a flat surface ($R\to\infty$, $h\to R$), expression (28) assumes the form obtained in [9].

Formula (28) makes it possible to determine the thickness of the entrained layer when the depth of the groove is constant. Under the conditions in which RHP operate, the depth of the groove decreases with increasing rotational speed because with increasing rotational speed the thickness of the layer outside the groove also increases whereas the amount of liquid in the pipe is constant, i.e., the value of h in (28) is a function of the rotational speed, and consequently also of δ_0. We write the expression correlating the amount of liquid in the annular layer, rotating together with the wall, with the amount of liquid in the groove. Taking into account the small value of δ_0, we assume here that the mean thickness of the layer outside the groove is equal to δ_0:

$$V - 2\pi Rl\delta_0 = \frac{(R-\delta_0)^2}{2}(2\varphi_Z - \sin 2\varphi_Z). \tag{29}$$

Taking into account the small values of φ_Z for RHP, we replace the function of $\sin 2\varphi_Z$ in (29) by two terms of the Taylor expansion and express the magnitude of h through the angle φ_Z:

$$h = R(1-\cos\varphi_Z) + \delta_0\cos\varphi_Z, \tag{30}$$

where

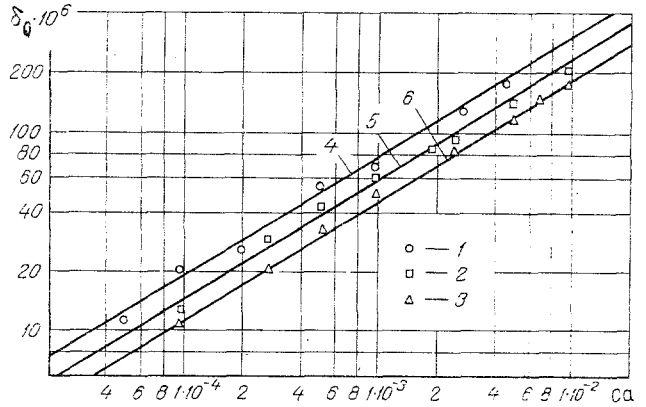

Fig. 3. Comparison of the results of the experimental investigation of the thickness of the entrained layer with dependence (32): 1) $\bar{\delta} = 0.25 \cdot 10^{-3}$ m; 2) $0.5 \cdot 10^{-3}$; 3) $1 \cdot 10^{-3}$; 4, 5, 6) calculation by Eq. (32) for $\delta = 0.25 \cdot 10^{-3}$, $0.5 \cdot 10^{-3}$, and $1 \cdot 10^{-3}$ m, respectively. $\bar{\delta}_0$, m; $Ca = \omega R \mu / \sigma$.

$$\varphi_z = \sqrt[3]{\frac{3(V - 2\pi R l \delta_0)}{2l(R - \delta_0)^2}}.$$

If we substitute h from (30) into Eq. (28) and change it into dimensionless form, we obtain:

$$Ca = \left(\frac{\Delta_0}{1.34}\right)^{3/2} \left[2 \frac{1 - (1 - \Delta_0)\cos \sqrt[3]{3\pi \frac{\bar{\Delta} - \Delta_0}{(1 - \Delta_0)^2}}}{A^2} + 1 \right]^{3/4}. \quad (31)$$

The numerical solution of Eq. (31) with respect to Δ_0 (in the range of change $A = 6 \cdot 10^{-2} - 12 \cdot 10^{-2}$, $\bar{\Delta} = 0.2 \cdot 10^{-2} - 5 \cdot 10^{-2}$, $\Delta_0 = 0 - 0.2\bar{\Delta}$) is approximated with an accuracy of 2.5% by the expression

$$\Delta_0 = 2 \cdot 10^{-2} \frac{Ca^{0.68}}{\bar{\Delta}^{0.36}} \exp(11.8A). \quad (32)$$

Thus formula (32) makes it possible to determine the thickness of the layer entrained by the inner surface of a cylindrical RHP as a function of the rotational speed, the geometric dimensions of the RHP, of the physical properties of the heat carrier and of its amount.

Figure 3 presents a comparison of the results of the experimental investigation of the thickness of the entrained layer with dependence (32). The working liquid was water. The experiments showed that formula (32) describes well the experimental data in the range of rotational speeds from the minimal speed to the speed at which waves begin to form on the surface of the groove.

NOTATION

r, φ, polar coordinates; x, y, z, orthogonal coordinates; g, acceleration of gravity; ρ, density; μ, dynamic viscosity; ν, kinematic viscosity; σ, specific surface energy; P, pressure; $a = (\sigma/\rho g)^{1/2}$, Laplace's capillary constant; v_ε, v_φ, components of the speed of the liquid; ω, angular speed of rotation; ω_B^{per}, ω_H^{per}, rotational speeds corresponding, respectively, to the upper and lower boundaries of the region of hysteresis; R, radius of the inner surface; R_{cr}, radius of curvature of the free surface of the liquid; R_{cr}^{st}, R_{cr}^{d}, radii of curvature determined by the equations of static and dynamic menisci, respectively; H_M, height of rise of the meniscus; h, depth of the groove; l, length of the pipe; V, volume of liquid in the pipe; $\bar{\delta} = V/2 \cdot \pi \cdot R \cdot l$, mean thickness of the layer of liquid; δ_m, maximum thickness of the layer; δ_0, thickness of the entrained thin layer; $\xi = \delta_m \sqrt{\delta}$; φ_m, angular coordinate of the maximum thickness of the layer; $Fr_c = \omega^2 R/g$, centrifugal Froude number; $Re = \omega(\bar{\delta})^2/\nu$, Reynolds number; $Ca = \omega R \mu/\sigma$, capillarity number; $\bar{\Delta} = \bar{\delta}/R$; $\Delta_0 = \delta_0/R$; $A = a/R$.

LITERATURE CITED

1. B. N. Krivosheev, M. P. Kukharskii, and V. D. Portnov, "Investigation of the heat transfer in a centrifugal heat pipe with optimized thickness of the layer of liquid," Tr. MÉI, No. 448, 32-35 (1980).
2. B. N. Krivosheev, M. P. Kukharskii, and V. D. Portnov, "Investigation of the heat transfer on the evaporative section of a rotating heat pipe at low rotational frequencies," Inzh.-Fiz. Zh., 37, No. 1, 39-43 (1979).
3. S. K. Zhuk and Yu. A. Khmelëv, "Experimental investigation of the distribution of temperature and of the intensity of heat exchange in centrifugal heat pipes, the shafts of heavy-duty electric motors," Promyshlennaya Teplotekh., 2, No. 3, 28-32 (1980).
4. A. I. Borisenko, O. N. Kostikov, V. I. Chumachenko, and A. I. Yakovlev, "Some results of the investigation of a centrifugal-axial heat pipe," in: Aerodynamics and Heat Transfer in Electrical Machines, Issue 3, Kharkov Aviation Inst. (1973), pp. 50-58.
5. J. A. Deiber and R. L. Cerro, "Viscous flow with a free surface inside a horizontal rotating drum. 1. Hydrodynamics," Izd. Eng. Chem., Fundam., 15, No. 2, 102-110 (1976).
6. B. Braun, "Beschreibung des Wärmeüberganges in dampfebeheizten, waagerecht rotierenden Trockenzylindern auf der Grundlage einer verfeinerten Analyse der Kondensatringströmung," in: Dok. Diss. Fak. Techn. Univ. Hannover (1977), pp. 114-121.
7. Yu. A. Khmelëv and A. S. Savchenko, "Installation for the production and experimental investigation of centrifugal heat pipes," in: Investigation of Processes of Heat and Mass Exchange [in Russian], Naukova Dumka, Kiev (1979), pp. 136-142.
8. A. J. Soroka and I. A. Tallmadge, "A test of the inertial theory for plate withdrawal," AIChE J., 17, No. 2, 505-510 (1971).
9. V. G. Levich, Physicochemical Hydrodynamics, Prentice-Hall (1962).

EXPERIMENTAL INVESTIGATION OF HEAT TRANSFER IN A CENTRIFUGAL HEAT PIPE WITH AN OPTIMIZED LAYER OF HEAT-TRANSFER AGENT

B. N. Krivosheev, M. P. Kukharskii, and V. D. Portnov

UDC 536.248.2

This paper describes a technique and gives results of experimental investigations of special features of heat transfer in the evaporator and condenser sections of a centrifugal heat pipe with optimized thickness of the layer of heat transfer agent.

Centrifugal heat pipes of various constructions [1] have found use recently to intensify cooling of rotary electric machinery. Internal heat transfer is somewhat higher in conical heat pipes than in cylindrical ones. However, it is a considerable technical problem to make long conical heat pipes ($l/d > 5$), especially with mass discharge. One way to intensify the heat transfer in cylindrical pipes is to use a condenser section of smaller diameter than that of the transfer and evaporator sections [2]. In a pipe of this construction the thickness of condensate layer increases in a stepwise manner towards the closed end of this section, and is therefore considerably less than in the simple cylindrical pipe, where it increases over the whole pipe length.

Another efficient way to intensify the heat transfer in a heat pipe is a device at the closed end of the evaporator section of the annular channel, for pouring away the excess condensate. Calculations presented in [3] have shown, for example, that if we fill a cylindrical heat pipe with heat-transfer agent for a design angular velocity of 70 rad/sec, and then increase the speed to 300 rad/sec, then up to 70% of the condensate is excess, and will lower the heat-transfer rate at low heat fluxes. If we provide an annular groove at the closed end of the evaporator section, the excess condensate will automatically flow into the groove, the result being that for any rotational speed the evaporator section will contain the minimal necessary (i.e., optimal) condensate layer.

Translated from Inzhenerno-Fizicheskii Zhurnal, Vol. 43, No. 5, pp. 775-780, November, 1982. Original article submitted August 28, 1981.

 0022-0841/82/4305-1242$07.50